Available online at www.CivileJournal.org

Civil Engineering Journal

(E-ISSN: 2476-3055; ISSN: 2676-6957)

Vol. 10, Special Issue, 2024
"Sustainable Infrastructure and Structural Engineering:
Innovations in Construction and Design"

Unified AI-Based Predictive Models for the Ultimate Capacity of Multi-Planar Gapped KK Steel Pipe Joints

Ahmed Kadry [1, 2*], Eslam El-Ganzoury [2], Abdel Salaam A. Mokhtar [2], Said Y. Aboul Haggag [2], Ahmed Ebid [1]

[1] *Structural Engineering and Construction Management Department, Faculty of Engineering and Technology, Future University in Egypt, Egypt.*

[2] *Structural Engineering Department, Faculty of Engineering, Ain Shams University, Cairo, Egypt.*

Received 04 July 2023; Revised 09 October 2023; Accepted 27 April 2024; Published 26 May 2024

Abstract

The multi-planar steel pipe joints are widely used in communication towers, industrial structures, and offshore platforms. The current design formulas consider this joint as a uniplanar joint and account for the multi-planar effect using empirical correction factors. Recent studies deal with this multi-planar joint as a 3D joint but considering certain loading conditions. Hence, the aim of this research is to develop more general AI-based predictive models for the ultimate capacity of multi-planar gapped KK steel pipe joints, considering both symmetric and asymmetric loading conditions. Three AI techniques were applied to a database of previously published works. These techniques are "Genetic Programming" (GP), "Artificial Neural Network" (ANN), and "Evolutionary Polynomial Regression" (EPR). The prediction accuracies of the developed AI models were compared against two previously published formulas. The results indicated that the developed AI models are much more accurate than the previously published formulas. Also, the results showed that both the ANN and EPR models have almost the same level of accuracy (about 92%), but the EPR model has the advantage of presenting a closed-form equation that could be implemented either manually or using software.

Keywords: Multi-Planar KK Joint; Ultimate Capacity; Unified Model; Symmetrical; Asymmetrical; Artificial Intelligence.

1. Introduction

Multi-planar steel pipe structures are 3D structures that are widely used in communication towers, industrial projects, and offshore platforms, as shown in Figure 1. They have the advantages of high-strength and lightweight. However, the difficulties of designing and constructing their joints in 3D space still need more advanced and detailed research.

Investigating the behavior of multi-planar steel tubular joints began in the early 80's when Makino et al. (1984) [1] investigated the ultimate capacity of tubular double K-joints under static loading. The authors conducted a series of experimental tests on 18 full-scale double K-joints with different gusset plate thicknesses and member diameters. The joints were subjected to axial loading, bending loading, or a combination of axial and bending loading. The results of the experimental tests showed that the ultimate capacity of the double K-joints was influenced by a number of factors, including the thickness of the gusset plate, the diameter of the members, the type of loading, and the ratio of axial to bending load. The authors developed a design formula for the ultimate capacity of tubular double K-joints based on the results of their experimental tests.

* Corresponding author: ahmed.shaheen@fue.edu.eg

http://dx.doi.org/10.28991/CEJ-SP2024-010-07

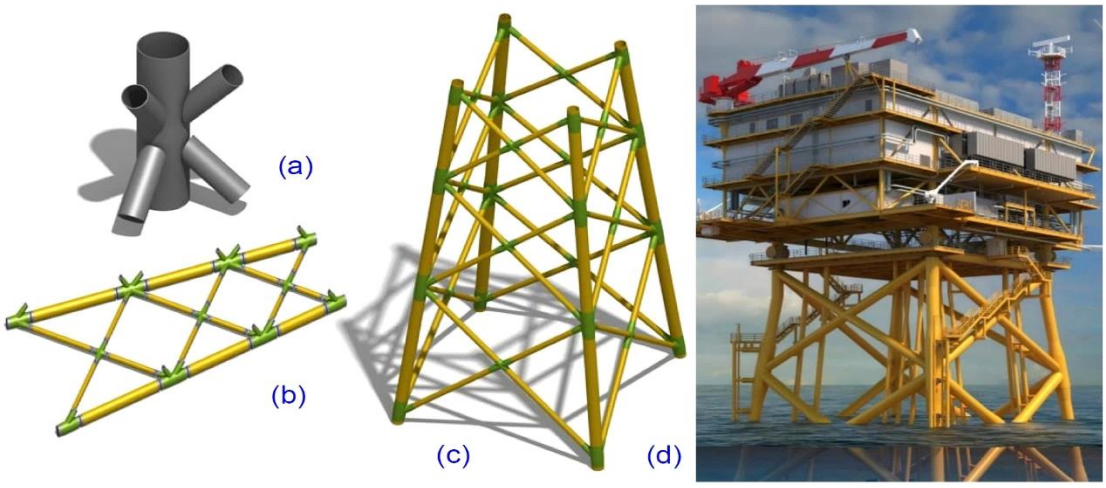

Figure 1. Implementation of multi-planar KK steel pipe joints in different types of structures a) Typical KK joint, b) Long spans, c) communication towers and d) offshore structures

Mouty & Rondal (1990) [2] studied the behavior of welded joints of circular hollow sections in triangular and quadrangular section beams under static loading. The authors conducted a series of experimental tests on 24 welded joints with different joint geometries, welding types, and loading conditions. The joints were subjected to axial loading, bending loading, or a combination of axial and bending loading. The results of the experimental tests showed that the behavior of the welded joints was influenced by the geometry of the joint, the type of welding, the loading condition, and the ratio of axial to bending load. The authors developed a design formula for the ultimate capacity of welded joints of circular hollow sections in triangular and quadrangular section beams based on the results of their experimental tests.

Makino et al. (1993) [3] investigated the ultimate behavior of diaphragm-stiffened tubular KK-joints. The authors conducted a series of experimental tests on 18 full-scale diaphragm-stiffened KK-joints with different gusset plate thicknesses, member diameters, and diaphragm stiffener configurations. The joints were subjected to axial loading, bending loading, or a combination of axial and bending loading. The results of the experimental tests showed that the diaphragm stiffeners significantly improved the strength and ductility of the KK-joints. The authors developed a design formula for the ultimate capacity of diaphragm-stiffened tubular KK-joints based on the results of their experimental tests.

Paul et al. (1992) [4] investigated the ultimate behavior of multi-planar TT- and KK-joints made of circular hollow sections. The author conducted a series of experimental tests on 12 full-scale multi-planar TT- and KK-joints with different member angles and loading conditions. The joints were subjected to axial loading, bending loading, or a combination of axial and bending loading. The results of the experimental tests showed that the multi-planar joints were more susceptible to buckling failure than the in-plane joints. The author also developed a design formula for the ultimate capacity of multi-planar TT- and KK-joints based on the results of his experimental tests.

Lee & Wilmshurst (1996) [5] conducted a parametric study of the strength of tubular multi-planar KK-joints. The authors developed a finite element model to simulate the behavior of the joints under axial loading. The finite element model was validated against the results of experimental tests conducted by other researchers. The authors then used the finite element model to investigate the effect of a number of factors on the strength of multi-planar KK-joints, including the thickness of the gusset plate, the diameter of the members, the angle between the members, and the loading condition. The results of the parametric study showed that the strength of the joints was influenced by all of the factors considered. The authors also developed a design formula for the strength of multi-planar KK-joints based on the results of their parametric study. Lee & Wilmshurst (1997) [6] investigated the strength of multi-planar tubular KK-joints under anti-symmetrical axial loading. The authors conducted a series of experimental tests on 12 full-scale multi-planar KK-joints with different member angles and loading conditions. The joints were subjected to anti-symmetrical axial loading, in which the two members were loaded in opposite directions. The results of the experimental tests showed that the strength of the joints was reduced under anti-symmetrical loading compared to symmetrical loading. The authors also developed a design formula for the strength of multi-planar KK-joints under anti-symmetrical axial loading based on the results of their experimental tests.

The previous studies laid the foundation for the basic understanding of the structural behavior of multi-planar steel pipe joints [1–6]. Recent studies in this field are focusing on more advanced aspects, including dynamic loading and fatigue analysis. Li et al. (2018) [7] investigated the behavior of a multi-planar joint in a transmission tower. The authors conducted a series of experimental tests on a full-scale multi-planar joint under static loading. The results of the experimental tests showed that the joint exhibited good strength and ductility. The authors also developed a design formula for the strength of multi-planar joints in transmission towers based on the results of their experimental tests.

Li & Lie (2019) [8] studied the strength reduction factors for cracked multi-planar tubular DT-joints. The authors developed a finite element model to simulate the behavior of the cracked joints under axial loading. The finite element model was validated against the results of experimental tests conducted by other researchers. The authors then used the finite element model to investigate the effect of crack size and location on the strength of multi-planar tubular DT-joints. The results of the study showed that the strength of the joints was significantly reduced by the presence of cracks. The authors also developed a set of strength reduction factors for cracked multi-planar tubular DT-joints based on the results of their study. Jiao et al. (2018) [9] conducted an experimental and numerical investigation of complex multi-planar welded tubular joints in umbrella-type space trusses with long overhangs. The authors conducted a series of experimental tests on four full-scale multi-planar welded tubular joints under static loading. The results of the experimental tests showed that the joints exhibited good strength and ductility. The authors also developed a finite element model to simulate the behavior of the joints. The finite element model was validated against the results of the experimental tests. The authors then used the finite element model to investigate the effect of different factors on the strength of the joints, such as the joint geometry, the loading condition, and the welding quality.

Zhao et al. (2019) [10] studied the out-of-plane flexural stiffness of unstiffened multi-planar CHS X-joints. The authors conducted a series of experimental tests on 12 full-scale unstiffened multi-planar CHS X-joints under out-of-plane bending loading. The results of the experimental tests showed that the out-of-plane flexural stiffness of the joints increased with the increase of the chord diameter and the decrease of the brace-to-chord angle. The authors also developed a design formula for the out-of-plane flexural stiffness of unstiffened multi-planar CHS X-joints based on the results of their experimental tests. Zavvar et al. (2021) [11] investigated the stress concentration factors of multi-planar tubular KT-joints subjected to in-plane bending moments. The authors developed a finite element model to simulate the behavior of the joints. The finite element model was validated against the results of experimental tests conducted by other researchers. The authors then used the finite element model to investigate the effect of different factors on the stress concentration factors of the joints, such as the joint geometry, the loading condition, and the welding quality. The results of the study showed that the stress concentration factors were highest at the weld toes and decreased with an increase in chord thickness.

Jiang et al. (2018) [12] developed a method for predicting the stress concentration factor distribution for multi-planar tubular DT-joints under axial loads. The proposed method is based on elastic theory and the concept of stress intensity factors. The authors validated the proposed method against the results of finite element analysis. The results showed that the proposed method can accurately predict the stress concentration factor distribution for multi-planar tubular DT-joints under axial loads. Liu et al. (2020) [13] studied the effects of brace-to-chord angle on the capacity of multi-planar CHS X-joints under out-of-plane bending moments. The authors conducted a series of experimental tests on 12 full-scale multi-planar CHS X-joints with different brace-to-chord angles under out-of-plane bending loading. The results of the experimental tests showed that the capacity of the joints decreased with the increase of the brace-to-chord angle. The authors also developed a design formula for the capacity of multi-planar CHS X-joints under out-of-plane bending moments based on the results of their experimental tests.

Kadry et al. (2022) [14] numerically examined un-stiffened multi-planar tubular KK joints and produced an accurate formula to calculate their capacities under symmetrical loads. Furthermore, Kadry et al. (2023) [15] developed another formula for the structural capacities of un-stiffened multi-planar tubular KK-gap joints under anti-symmetric loading.

Currently, various guides and codes addressed the design of uniplanar and multi-planar joints, such as the CIDECT manual [16], Eurocode 3 (2005) [17], Brazilian NBR 16239 (2013) [18], and Wardenier et al. (2010) [19]. Simulations have been used to determine the mechanical behavior of joints, which are commonly employed. The most recent are IIW (2012) [20] and ISO 14346 (2013) [21].

1.1. Objective

The survey of previous references showed that most design codes [16–21] considered the traditional design method where the multi-planar joint is designed as a uni-planar joint, then some empirical correction factor is used to account for the multi-planar effect. Which is not an accurate method. On the other hand, the recent proposed design methods [7–15] considered the multi-planar joint as a 3D structure; however, they considered a certain loading condition, which limits the applicability of their developed design formulas.

Hence, the main objective of this research is to develop a more general structural capacity formula for multi-planar gapped KK steel pipe joints, considering both symmetrical and symmetrical loading conditions.

2. Research Methodology

The methodology of this research started with collecting databases for multi-planar gapped KK steel pipe joint test results from previously published works. Then the collected data are statistically analyzed and used to train and validate three different AI models to predict joint capacity. Finally, the accuracy of the developed models was compared with

previous studies. Figure 2 presents the described framework graphically. Each step of the considered methodology is described in detail in the next paragraphs.

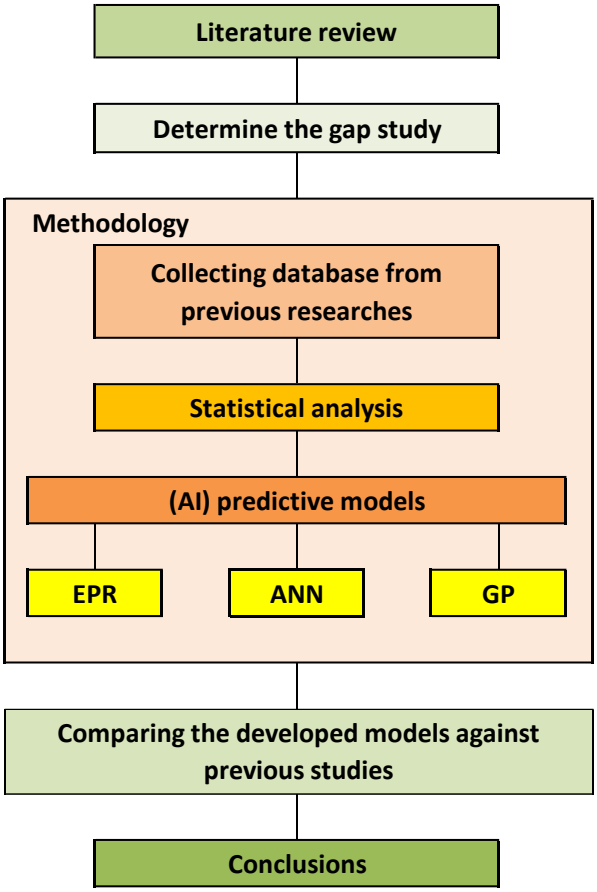

Figure 2. Framework of current study

2.1. Database

381 records of experimentally verified for FEM test results for multi-planar gapped KK steel pipe joints were collected verified were collected [14, 15]. Each record contains the following data:

- gl/Dc Local slenderness in the longitudinal direction;
- tc/gt Local slenderness in the transverse direction;
- tc/Dc Global slenderness of chord;
- tb/Db Global slenderness of brace;
- $\sigma u/Fy$ Normalized ultimate stress of chord;
- Sin(θ) (θ) is the angle between bracing and cord, in this research, it will be considered positive for symmetric loading and negative for asymmetric loading

The previous terms are defined in the abbreviation section and graphically illustrated in Figure 3.

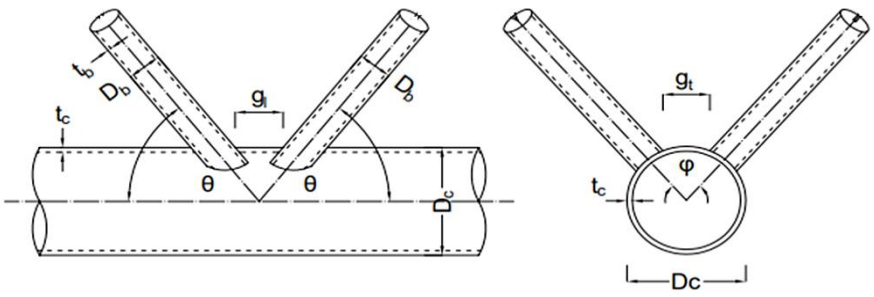

Figure 3. Geometrical configurations of multi-planar gapped KK steel pipe joint

The collected records were divided into training set (300 records) and validation set (81 records). The Appendix includes the complete dataset, while Table 1 and 2 summarizes their statistical characteristics and the Pearson correlation matrix. Finally, Figure 4 shows the histograms for both inputs and outputs.

Table 1. Statistical analysis of collected database

	Sin(θ)	gl/Dc	gc/gt	tc/Dc	tb/Db	σu/Fy
Training set						
Min.	-0.97	0.15	0.03	0.01	0.03	0.05
Max.	0.97	0.57	0.37	0.06	0.17	0.24
Avg.	-0.07	0.34	0.09	0.03	0.09	0.09
SD	0.85	0.05	0.05	0.01	0.02	0.03
VAR	-11.34	0.15	0.54	0.28	0.16	0.33
Validation set						
Min.	-0.97	0.15	0.03	0.01	0.04	0.05
Max.	0.97	0.48	0.37	0.04	0.14	0.21
Avg.	-0.12	0.35	0.09	0.03	0.09	0.09
SD	0.86	0.05	0.05	0.01	0.02	0.04
VAR	-7.22	0.16	0.53	0.32	0.17	0.38

Table 2. Pearson correlation matrix

	Sin(θ)	gl/Dc	tc/gt	tc/Dc	tb/Db	σu/Fy
Sin(θ)	1.00					
gl/Dc	0.10	1.00				
tc/gt	-0.20	-0.18	1.00			
tc/Dc	-0.04	0.27	0.56	1.00		
tb/Db	0.07	0.23	0.13	0.63	1.00	
σu/Fy	-0.04	0.14	0.70	0.71	0.26	1.00

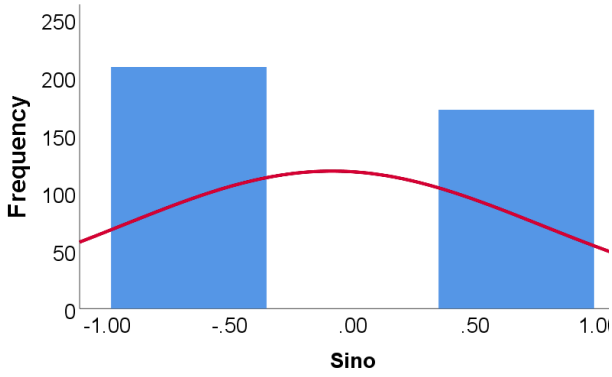

Sin(θ)

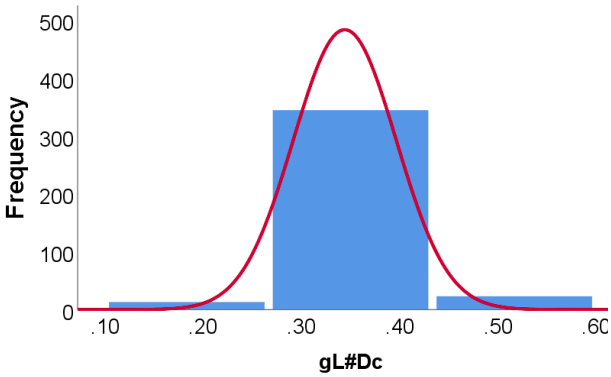

gl/Dc

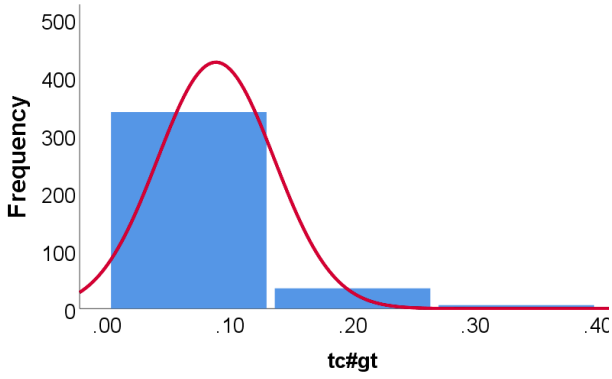

tc/gt

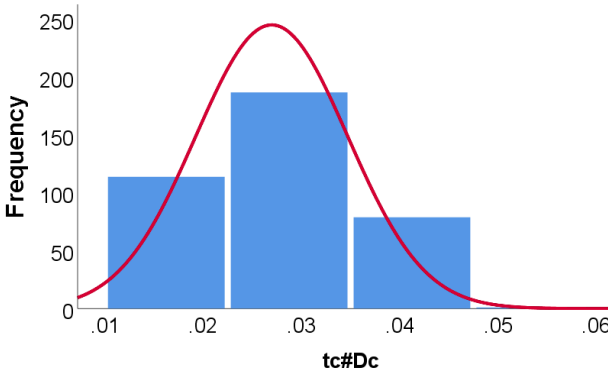

tc/Dc

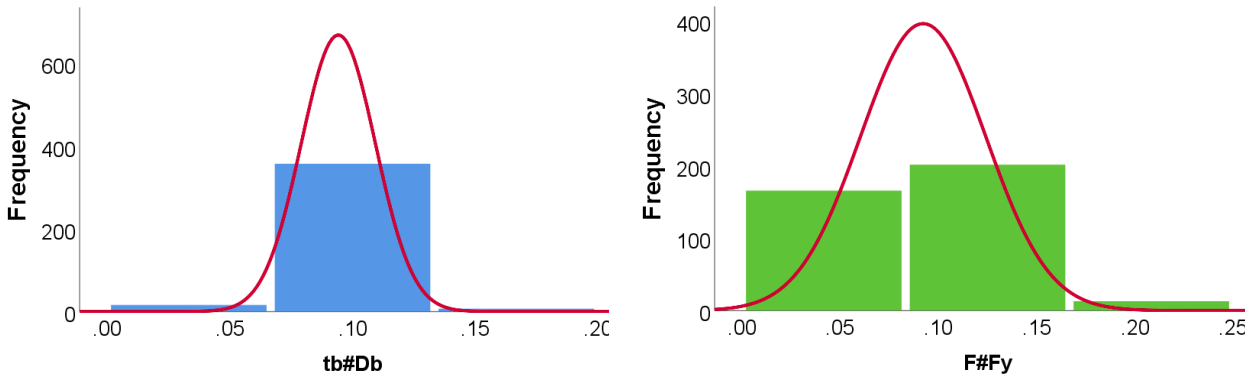

tb/Db σu/Fy

Figure 4. Distribution histograms for inputs (in blue) and outputs (in green)

2.2. (AI) Predictive Models

Three different Artificial Intelligent (AI) techniques were used to predict the Normalized ultimate stress of chord (σu/Fy) for KK multi-planar joint under symmetric or asymmetric loading using the collected database. These techniques are "Genetic programming" (GP), "Artificial Neural Network" (ANN), and "Evolutionary Polynomial Regression" (EPR). All three developed models were used to predict (σu/Fy) using angle between bracing and cord (θ), Local slenderness in longitudinal and transverse directions (gl/Dc & tc/gt), Global slenderness of chord & braces (tc/Dc & tb/Db).

Each model of the three developed models was based on a different approach (evolutionary approach for GP, mimicking biological neurons for ANN, and optimized mathematical regression technique for EPR). However, prediction accuracy was evaluated for all developed models regarding the Sum of Squared Errors (SSE).

The following section discusses the results of each model. The Accuracies of developed models were evaluated by comparing the (SSE) between predicted and calculated normalized ultimate stress values.

2.2.1. (GP) Model

The developed GP model has five levels of complexity. The population size, survivor size, and number of generations were 100 000, 30 000, and 150, respectively. Equation 1 presented the output formula for (σu/Fy), while Figure 5(a) showed its fitness. The average error % of the total dataset is (15.8%), while the (R^2) value is (0.805).

$$\frac{\sigma u}{Fy} = \left(\frac{tc}{Dc}\right)\left(\frac{Db}{tb}\right)^{\frac{2}{3}}\left(\frac{tc}{gt}\right)^{\frac{1}{4}}\left(\frac{Dc}{gl}\right)^{\frac{1}{8}}\left(\frac{0.93}{|Sin(\theta)|}\right)^{\frac{3}{2}} \quad (1)$$

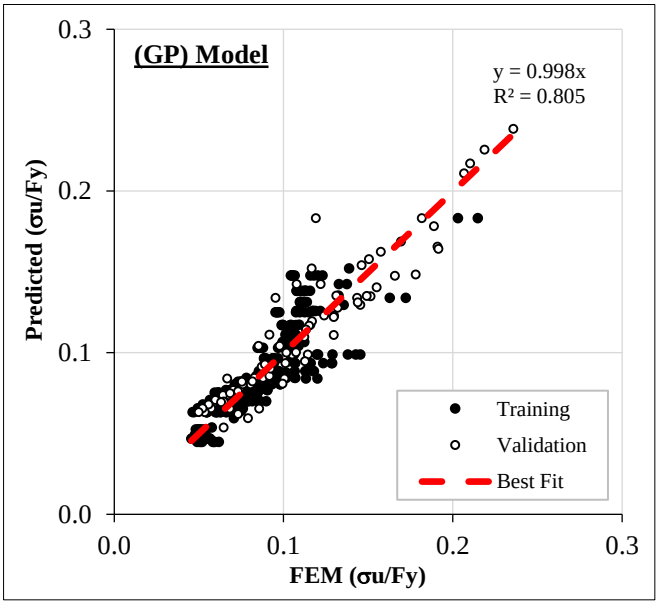

(a)

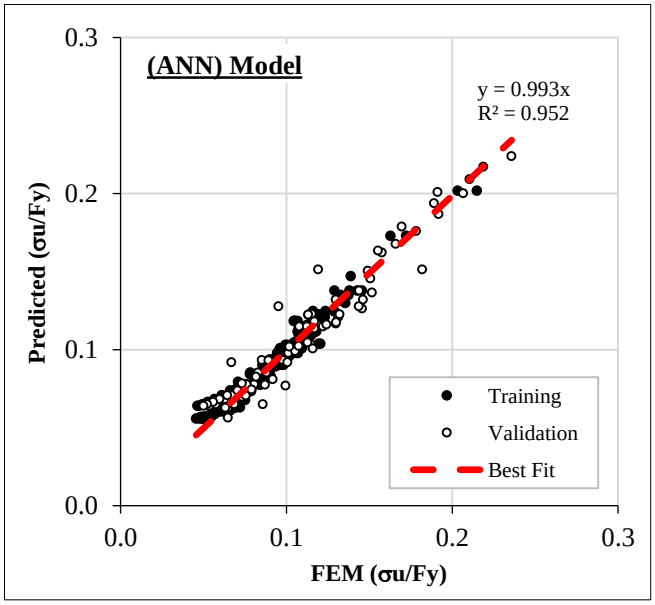

(b)

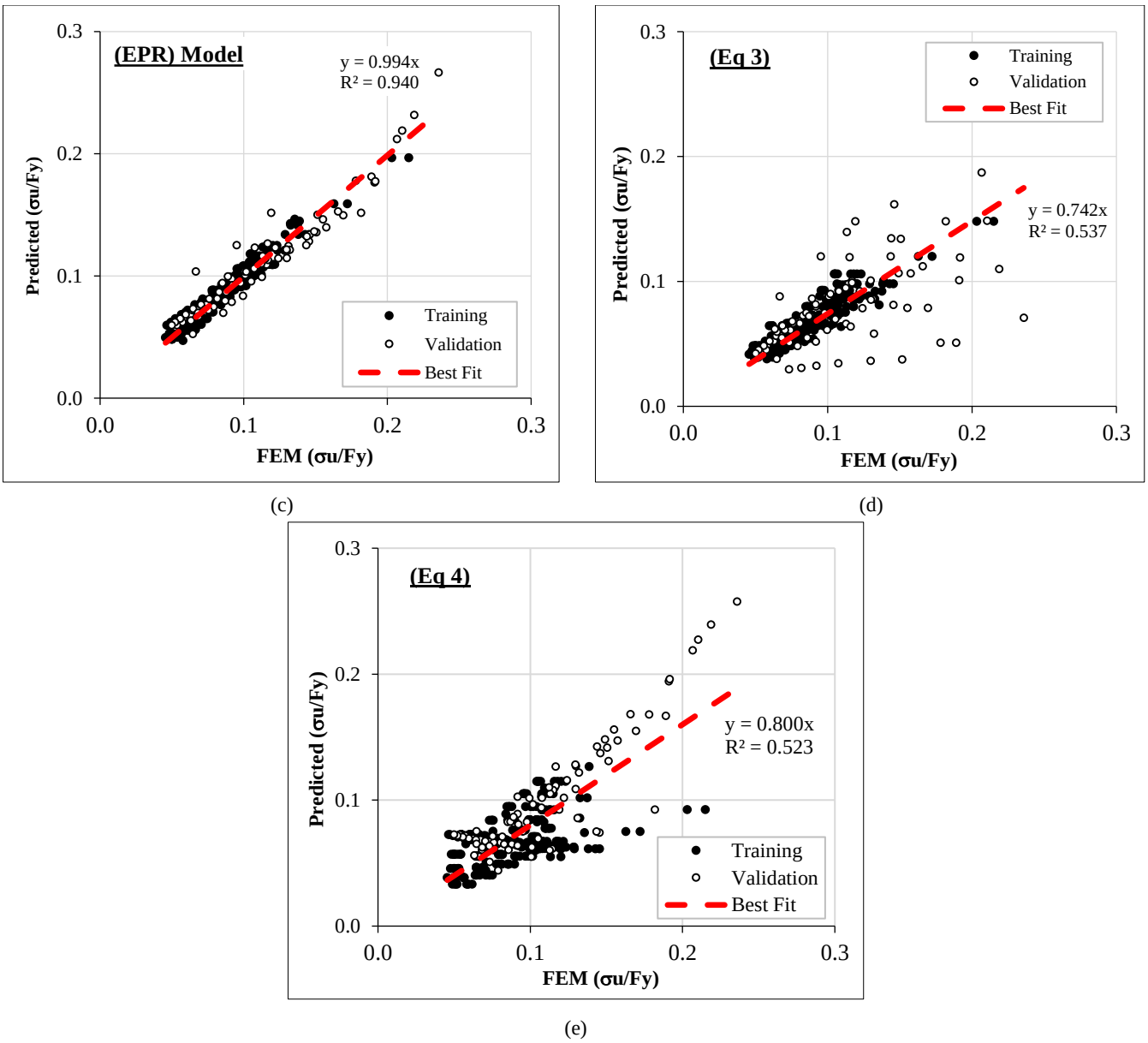

Figure 5. Relation between predicted and calculated (σu/Fy) values using the developed models and previous formulas

2.2.2. (ANN) Model

An (ANN) model was developed to predict (σu/Fy) values using the normalization method (-1.0 to 1.0), activation function (Hyper Tan), and "Back propagation" (BP) training algorithm. The used network layout is illustrated in Figure 6, while the weight matrix is shown in Table 3. The average error % of the total dataset is (7.3%), and the (R^2) value is (0.952) respectively. The relative importance values for each input parameter are illustrated in Figure 7, which indicates that the bracing angle in the longitudinal direction (θ) and the local slenderness in the transverse direction (tc/gt) are the most influential parameters. The global slenderness of the chord & braces (tc/Dc & tb/Db) and the local slenderness in the longitudinal direction (gl/Dc) come in the end. The relations between calculated and predicted values are shown in Figure 5(b).

Table 3. Weights matrix for the developed ANN

	H1	H2	H3	H4	H5	
(Bias)	1.357	0.122	-0.667	0.377	-0.493	
Sin(θ)	-1.986	-0.335	0.108	0.990	-0.030	
gl/Dc	0.129	0.054	0.024	-0.058	0.322	
tc/gt	0.187	-0.464	-0.356	0.042	-0.975	
tc/Dc	-0.034	0.084	0.114	0.106	0.448	
tb/Db	0.216	0.131	0.112	0.017	0.145	
	H1	**H2**	**H3**	**H4**	**H5**	**(Bias)**
σu/Fy	1.368	-0.930	0.764	1.213	0.385	-0.382

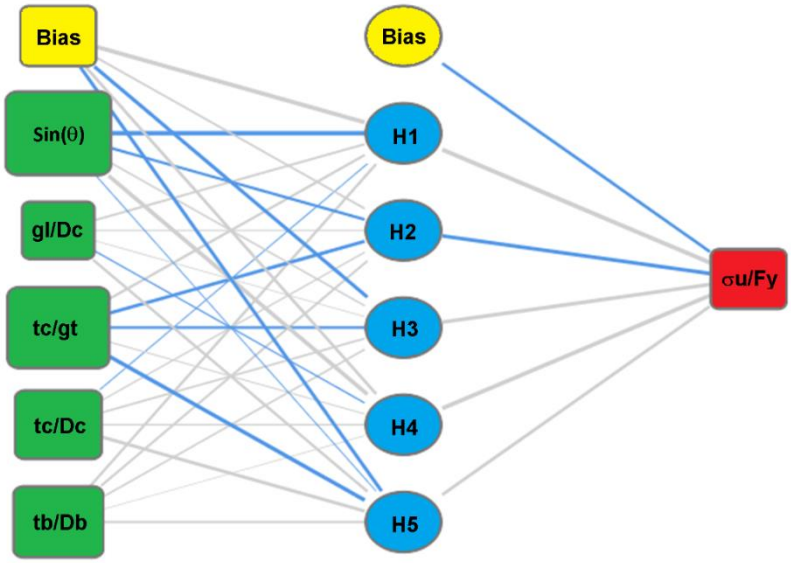

Figure 6. 5 Layout for the developed ANN model

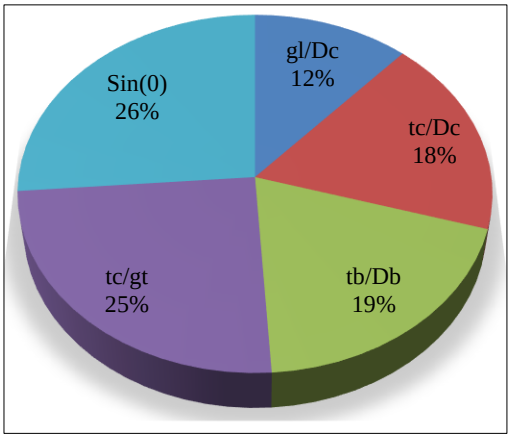

Figure 7. Relative importance of input parameters

2.2.3. (EPR) Model

Finally, the developed EPR model was quadratic level polynomial. For 5 inputs, there are 21 possible terms (15+5+1=21) as follows:

$$\sum_{j=1}^{j=5}\sum_{i=1}^{i=5} X_j . X_i + \sum_{i=1}^{i=5} X_i + C \quad (2)$$

GA technique was applied to these 21 terms to select the most effective ten terms to predict the value of (σu/Fy). The output is illustrated in Equation 3, and its fitness is shown in Figure 7 Figure 5(c). The average error % and (R^2) values were (8.2% & 0.940) respectively.

$$\frac{\sigma_u}{Fy} = \left(\frac{Dc}{28.5\ gl}\right)^2 + \frac{1}{Sin(\theta)}\left(\frac{gL}{15\ Dc} - \frac{Db}{623\ tb} + \frac{1}{32.3\ Sin(\theta)}\right) - \frac{Sin(\theta)\ tb}{18.6\ Db} + \frac{gL\ gt}{56.7\ Dc\ tc} + \frac{tc}{1.85\ gt} - \frac{gt}{130.6\ tc} + \frac{gt}{5.5\ Dc} - \frac{1}{19.1} \quad (3)$$

2.3. Comparison with Previous Studies

The prediction accuracy of the joint capacity using the developed (AI) predictive models were compared against two formulas form previously published as shown in Equation 4 [14], Equation 5 [15].

$$\frac{\sigma u}{Fy} = \frac{1.25\cos(\varphi/2)}{Sin(\theta)} \sqrt[3]{\left(\frac{g_l}{D_c}\right)^3 \frac{t_c}{g_t}\left(\frac{t_c}{D_c}\frac{D_b}{t_b}\right)^2} \quad (4)$$

$$\frac{\sigma u}{Fy} = \frac{0.33}{Sin(\theta)}\left(\frac{t_c}{g_t}\right)\sqrt[6]{\left(\frac{t_b}{D_b}\right)\left(\frac{g_t}{g_l}\right)\left(\frac{D_c}{t_c}\right)^2} \quad (5)$$

Equation 4, 5 were developed for symmetrical and asymmetrical loading conditions respectively. The fitness of these formulas is shown in Figure 5 (d, e). The average error % and (R^2) values were (32.4% & 0.537) and (30.8%, 0.523) respectively.

3. Results and Discussion

As mentioned in the methodology section, three (AI) predictive models were developed to predict the normalized ultimate stress (σu/Fy), besides that, two predictive formulas from earlier researches were used for comparison. For these five predictive models, "Sum of Squared Error" (SSE), Average error percent (Avg. Error %) and "Determination factor" (R2) were calculated and summarized in Table 4. Moreover, the relation between the FEM and predicted capacities for the five predictive models were graphically presented in Figure 5. Finally, a comparison between the accuracies of the five models were graphically presented using Taylor chart in Figure 8.

Table 4. Accuracies of developed models and pervious formulas

Technique	Model	SSE	Avg. Error %	R^2
GP	Eq. 1	0.080	15.8%	0.805
ANN	Figure 6, Table 3	0.017	7.3%	0.952
EPR	Eq. 3	0.022	8.2%	0.940
[14]	Eq 4	0.339	32.4%	0.537
[15]	Eq 5	0.306	30.8%	0.523

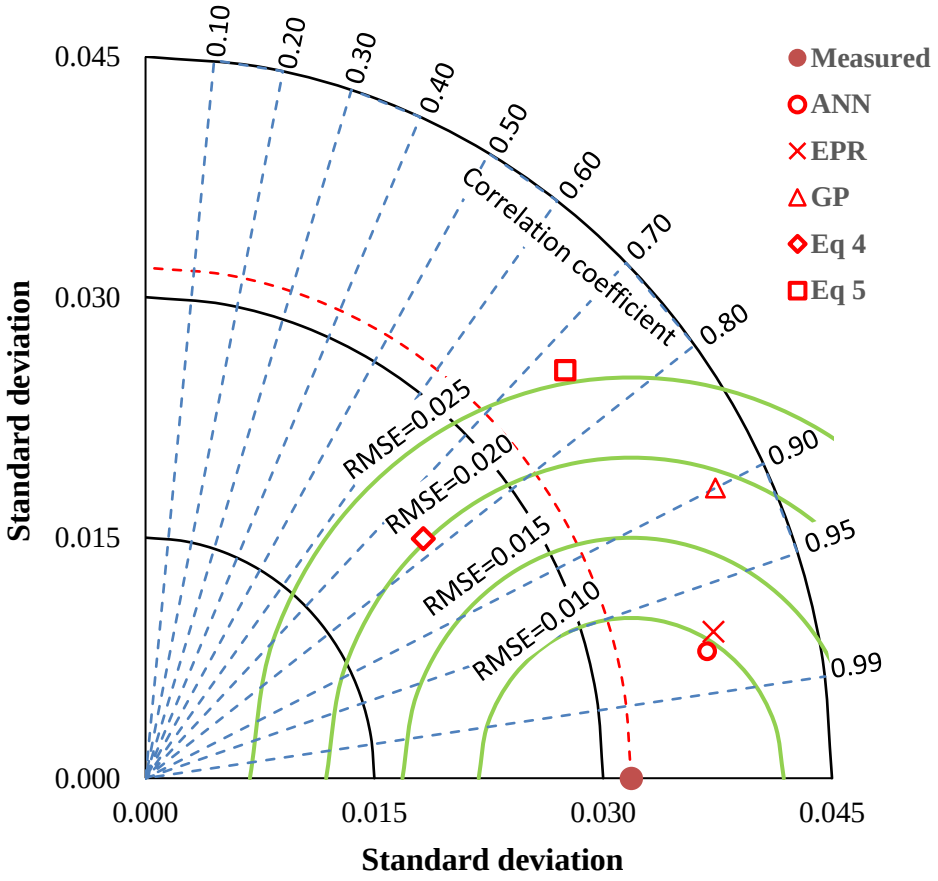

Figure 8. Comparing the accuracies of the developed models and previous formulas using Taylor chart

The presented results of this research in Table 4 and Figures 5 and 8 showed that the considered previous work formulas (Equation 4, 5) showed very low accuracy (about 70%) because they were developed considering a single loading condition (either symmetrical or asymmetrical), which is the limitation that should be overcome in this research.

Regarding the developed AI models, although the GP model presents the simplest and least accurate one with an accuracy of 84%, but it is still much better than Equations 4 and 5. Using the absolute value of sin(q) in Equation 1 means that the joint has the same ultimate capacity under both symmetrical and asymmetrical loading conditions; this major defect may be the cause of the high error percent.

On the other hand, the ANN model presents the most accurate model, with an accuracy of 93%. This is due to the high nonlinearity of the activation function (Hyper Tan), which allowed the network to capture the nonlinear behavior of the joint. However, the ANN model is too complicated to be used manually; it must be calculated using special software. This gives the EPR a middle place between the GP and ANN models. It is simpler than ANN but more

complicated than GP. Also, it is more accurate than GP but less accurate than ANN. In addition, it is a closed-form formula that could be used manually or embedded in software.

Regarding the impact of each input on the capacity of the joint, the correlation matrix in Table 2 indicated that both the local and global slenderness ratios of the cord had the major impact on the joint capacity, followed by the global slenderness ratio of the bracing, while the angle between the bracing and the cord had a neglected impact. This statistical ranking does not match the outputs of the ANN model (the most accurate model), which gives all the inputs almost the same relative importance (about 18%) with some extra importance to the angle between bracing and cord (about 26%), as shown in Figure 7. Both the GP and EPR models agreed with the ANN model since Equations 1 and 2 included all the inputs.

4. Conclusion

The outcomes of this research indicated that the proposed methodology of using collected FEM test results to train and validate AI predictive models fulfilled the objective of this research. And the three developed predictive models successfully estimated the structural capacity of the multi-planar KK gapped joint under symmetrical and asymmetrical loading conditions. Each of the developed models has its advantages and disadvantages. The GP model is the simplest but the least accurate; the ANN model is the most accurate but the most complicated; and EPR has average accuracy and complexity. The three models indicated that all inputs had almost the same impact on joint capacity, with a slightly higher importance given to the angle between barking and cord. Comparing the accuracies of the developed AI models with previous work formulas showed that the prediction accuracy enhanced from 70% to 93%, which is expected because the previous work formulas were developed considering a single load condition, and this is the innovation point of this research. Finally, the validity of the developed models is limited by the considered range of values for each input, and they should be verified beyond these ranges. For further studies, it is recommended to extend the applicability of these predictive models to include a wider range of input values and more multi-planar joint geometry, such as overlapped joints and stiffened joints.

5. Abbreviations

Db	Brace tube diameter (mm)	Dc	Chord tube diameter (mm)
gl	Longitudinal gap between brace toes (mm)	gt	Transverse gap between brace toes (mm)
tb	Brace tube wall thickness (mm)	tc	Chord tube wall thickness (mm)
φ	Angle between K-planes (degree)	θ	Angle between brace and chord (degree)
Fy	Yield stress (MPa)	$\sigma\underline{u}$	Normal stress in cord at failure (MPa)

6. Declarations

6.1. Author Contributions

Conceptualization, S.Y.A.H.; methodology, A.E.; formal analysis, A.K.; investigation, A.E.; data curation, E.E.; writing—original draft preparation, A.K.; supervision, A.S.A.M. All authors have read and agreed to the published version of the manuscript.

6.2. Data Availability Statement

The data presented in this study are available in the article.

6.3. Funding

The authors received no financial support for the research, authorship, and/or publication of this article.

6.4. Conflicts of Interest

The authors declare no conflict of interest.

7. References

[1] Makino, Y., Kurobane, Y., & Ochi, K. (1984). Ultimate Capacity of Tubular Double K-Joints. Proc. 2nd Int. Inst. of Welding Con, 451–458. doi:10.1016/b978-0-08-031156-2.50037-3.

[2] Mouty, J., & Rondal, J. (1993). Study of the behavior under static load of welded assemblies of circular hollow sections in beams of triangular and quadrangular sections. EUR(Luxembourg). (In French).

[3] Makino, Y., Kurobane, Y., & Paul, J. C. (1993). Ultimate Behavior of Diaphragm-Stiffened Tubular Kk-Joints. CRC Press, Boca Raton, United States.

[4] Paul, J. C. (1992). The ultimate behavior of multi-planar TT- and KK-joints made of circular hollow sections. PhD thesis, Kumanmoto University, Kumanmoto, Japan.

[5] Lee, M. M. K., & Wilmshurst, S. R. (1996). Parametric Study of Strength of Tubular Multiplanar KK-Joints. Journal of Structural Engineering, 122(8), 893–904. doi:10.1061/(asce)0733-9445(1996)122:8(893).

[6] Lee, M. M. K., & Wilmshurst, S. R. (2022). Strength of multiplanar tubular KK-joints under anti-symmetrical axial loading. Tubular Structures VII, 149–156, Routledge, Milton Park, United Kingdom. doi:10.1201/9780203735008-24.

[7] Li, F., Deng, H. Z., Cai, Q., Dong, J. Y., & Fu, P. C. (2018). Experiment and design investigation of a multi-planar joint in a transmission tower. Journal of Constructional Steel Research, 149, 78–94. doi:10.1016/j.jcsr.2018.07.008.

[8] Li, T., & Lie, S. (2019). Strength Reduction Factors for Cracked Multi-planar Tubular DT-joints. KSCE Journal of Civil Engineering, 23(1), 307–320. doi:10.1007/s12205-018-0547-z.

[9] Jiao, J., Ma, X., Lei, H., & Chen, Y. F. (2018). Experimental and Numerical Study on Complex Multi-planar Welded Tubular Joints in Umbrella-Type Space Trusses with Long Overhangs. International Journal of Steel Structures, 18(5), 1525–1540. doi:10.1007/s13296-018-0064-4.

[10] Zhao, B., Liu, C., Wu, H., Ge, Y., Yang, J., & Yi, Q. (2019). Study on out-of-plane flexural stiffness of unstiffened multi-planar CHS X-joints. Engineering Structures, 188, 137–146. doi:10.1016/j.engstruct.2019.03.023.

[11] Zavvar, E., Hectors, K., & De Waele, W. (2021). Stress concentration factors of multi-planar tubular KT-joints subjected to in-plane bending moments. Marine Structures, 78, 103000. doi:10.1016/j.marstruc.2021.103000.

[12] Jiang, Y., Yuan, K., & Cui, H. (2018). Prediction of stress concentration factor distribution for multi-planar tubular DT-joints under axial loads. Marine Structures, 61, 434–451. doi:10.1016/j.marstruc.2018.06.017.

[13] Liu, C., Zhao, B., Yang, J., Yi, Q., Yao, Z., & Wu, J. (2020). Effects of brace-to-chord angle on capacity of multi-planar CHS X-joints under out-of-plane bending moments. Engineering Structures, 211, 110434. doi:10.1016/j.engstruct.2020.110434.

[14] Kadry, A. A., Ebid, A. M., Mokhtar, A. salaam A., El-Ganzoury, E. N., & Haggag, S. Y. A. (2022). Parametric study of Unstiffened multi-planar tubular KK-Joints. Results in Engineering, 14. doi:10.1016/j.rineng.2022.100400.

[15] Kadry, A. A., Ebid, A. M., El-Ganzoury, E. N., Aboul Haggag, SaidY., & A. Mokhtar, A. (2023). Capacity of unstiffened multi-planar tubular KK-gap joints under anti-symmetric loading. Results in Engineering, 18, 101092. doi:10.1016/j.rineng.2023.101092.

[16] Wardenier, J., Kurobane, Y., Packer, J. A., Van der Vegte, G. J., & Zhao, X. L. (2008). Design guide for circular hollow section (CHS) joints under predominantly static loading. Steel & Composite Structures, Construction with hollow steel sections, Geneva, Switzerland.

[17] EN 1993-1-8. (2005). Eurocode 3: Design of steel structures – Part 1-8: Design of joints. European Committee for Standardization, Brussels, Belgium.

[18] NBR 16239. (2013). Design of steel and composite structures for buildings using hollow sections. Associação Brasileira de Normas Técnicas (ABNT), São Paulo, Brazil.

[19] Wardenier, J., Packer, J. A., Zhao, X. L., & Van der Vegte, G. J. (2002). Hollow sections in structural applications. Rotterdam. Bouwen met staal, Zoetermeer, Netherlands.

[20] IIW XV-1402-12. (2012). Static design procedure for welded hollow section joints – Recommendations. International Institute of Welding, Paris, France.

[21] ISO 14346:2013. (2013). Static Design Procedure for Welded Hollow-Section Joints - Recommendations. International Standards Organization (ISO), Geneva, Switzerland.